The GRNN and the RBF Neural Networks for 2D Displacement Field Modelling. Case study: GPS Auscultation Network of LNG reservoir (GL4/Z industrial complex – Arzew, Algeria)

Bachir GOURINE, Habib MAHI, Amar KHOUDIRI and Youcef LAKSARI, Algeria

Key words: Displacement field, Strain tensor, Artificial Neural Network, Radial Basis Function (RBF), Generalized Regression Neural Networks (GRNN)

SUMMARY

The analysis of the horizontal geodetic network for the crustal movement estimation is generally based on the vector displacements or on the strain tensors. These latter are independent of the reference frame and describe well the deformation. However, the strain tensors are influenced by the configuration of the selected elementary figures which are obtained from the geodetic points. To overcome this drawback, the regular grid presents an alternative solution for homogeneous and continuous representation of network deformation under condition to choose an optimal interpolator. In this context, the interpolation techniques based neural networks offer more advantages that the standard ones. This paper proposes to investigate the ability of the Generalized Regression Neural Network (GRNN) and the Radial Basis Functions Neural Network (RBFNN) for modelling of displacements field. The experimentations were conducted on a set of 56 points measured around the underground reservoir of GL4/Z industrial complex (Arzew – Algeria), by two GPS observation campaigns over 6-years period (2000-2006). The results and comparison with the standard techniques developed for the grid displacement interpolation, such as, the polynomial fitting and the nearest neighbours indicate that the GRNN achieves higher accuracy estimation than the others.

The GRNN and the RBF Neural Networks for 2D Displacement Field Modeling. Case study: GPS Auscultation Network of LNG reservoir (GL4/Z industrial complex – Arzew, Algeria)

Bachir GOURINE, Habib MAHI, Amar KHOUDIRI and Youcef LAKSARI, Algeria

1. INTRODUCTION

When one seeks to detect and estimate movements of the ground on the Earth surface, either tectonic motion (active faults) or landslides or even auscultation of structures presenting a risk of destabilization such as bridges, industrial sites and dams (Gikas and Sakellariou, 2008a; 2008b), the methodology employed consists in establishing a precise and homogeneous geodetic network, covering the area of study. The network benchmarks are determined thanks to terrestrial and/or space positioning techniques (GNSS). The reiteration of the observations of the same network, after a certain time, permits to detect the movements appeared during this period, by coordinate's variation estimation.

There are two methods to evaluate these movements (Welsch, 1983; Prescott et al., 1979): vector-displacements and strain tensors. Considered as gradient of the displacement field, the strain tensors represent a very efficient tool to perform the deformation computation and can be very helpful to analyse the behaviour of the studied area. Unlike to the vector-displacements, they are independent of any reference frame which makes very delicate the interpretation of the movements.

Nevertheless, the strain tensors computation depends on the configuration of the selected elementary figures formed from the geodetic points. This constraint makes difficult the interpretation of the results obtained (Merbah et al., 2005). The solution consists in evaluating these tensors according to regular grid, in order to allow homogenous and continuous representation of deformation in any point of the area (Kasser and Thom, personnel paper). In this case, many traditional interpolation methods are used usually for displacement field modelling, such as polynomial fitting, nearest neighbours, spline, etc.

Since a decade, the artificial neural network (ANN) has been applied in diverse fields of geodesy (Miima et al., 2001; Schuh et al., 2002). As for geoid model determination, several studies have been realised (Lin, 2009; Gullu et al., 2011). ANN was employed as an approximator for crustal velocity field (Moghtased-Azar and Zaletnyik, 2009) and it was adapted for structural behaviour modelling.

The objective of the present paper is to use Generalized Regression Neural Network (GRNN) in generating the displacement field, for deformation estimation, as alternative method to the traditional interpolation methods. The study area concerns the ground of the Liquefied Natural Gas (LNG) underground reservoir (GL4/Z industrial Complex – Arzew, ALGERIA).

Two GPS observation campaigns, over 6 year period (2000 - 2006), were carried out on the auscultation network composed of 56 points. A comparison between classical interpolators and the new approach based on GRNN was done, in terms of root mean square error (RMSE)

of displacement differences on testing points. Finally, a deformation significance analysis was performed with deformability and reliability concepts.

2. METHODOLOGY

2.1 Displacement and Deformation modelling

The 2D local displacement field around a given point *M(x,y)*, is simply the difference of coordinates of this point between two epochs, as:

$$U(x,y)=\begin{pmatrix} u(x,y) \\ v(x,y)) \end{pmatrix} \quad (1)$$

This representation of deformation mainly suffers from dependence to reference frame.
The strain tensor *E(x, y)* is defined as the gradient of the displacement field and is expressed by (Seemkooei et al., 2001 ; Vanicek et al., 2001):

$$E(x,y)=\frac{\partial U(x,y)}{\partial X}=\begin{pmatrix} \frac{\partial u}{\partial x}(x,y) & \frac{\partial u}{\partial y}(x,y) \\ \frac{\partial v}{\partial x}(x,y) & \frac{\partial v}{\partial y}(x,y) \end{pmatrix}=\begin{pmatrix} e_{ux} & e_{uy} \\ e_{vx} & e_{vy} \end{pmatrix} \quad (2)$$

This matrix gathers most of the information of displacement field behaviour. However, the interpretation of such a tensor is not obvious but its decomposition may help extracting some characteristic quantities known as deformation primitives. These later represent the deformation, in a more meaningful way. They are usual in material characteristics and mechanics. In this study, the deformation primitives have been chosen are positive scalars, growing with deformation amplitude, as:

- Total dilatation : $\lambda=\frac{1}{2}\left(e_{ux}+e_{vy}\right)$;
- Total shear : $\gamma=\gamma_{xy}=\gamma_{yx}=\frac{1}{2}\sqrt{\left(e_{ux}-e_{vy}\right)^2+\left(e_{uy}+e_{vx}\right)^2}$.
- Differential rotation or twist: $\delta\omega=\frac{1}{2}\left(e_{uy}-e_{vx}\right)-\Omega=\omega-\Omega.$

where Ω is rigid rotation which affects the whole area. It represents the global rotation which corresponds to average value of rotations ω on points of the network.

2.2 Interpolation methods

Generally, the monitoring geodetic points are geographically distributed with heterogeneous manner, which makes difficult the interpretation of deformation. The use of regular grid is the best way to get a homogenous and continuous representation of the displacement/deformation field on the whole area. In this case, the application of an interpolation function based on the geodetic points permits to approximate the displacement on each node *i* (x_i, y_i) of the grid. Among the different classical interpolation methods used for generating of displacement field, we present the two most popular.

2.2.1 Polynomial method

Polynomial interpolation is the most known one-dimensional interpolation method. Its advantages lies in its simplicity of realization and the good quality of interpolants obtained from it. The basic idea of these methods is to find constant coefficients by the reference points (training points) to form the displacement field model and calculates the unknown values for new points using these constant coefficients. The polynomial function is expressed by:

$$F(x,y)=\sum_{i=0}^{n}\sum_{j=0}^{n}a_i x^i y^j \tag{3}$$

Where, a_i and n are the coefficient and degree of the polynomial function, respectively. x, y are the coordinates of training points.

2.2.2 Nearest Neighbour method

The Nearest Neighbour method creates a surface which is optimized for a neighbourhood. The reference points in a neighbourhood can be weighted by their distances from the prediction location with inverse distance weighting. The equation of this interpolator, in the case of displacement in x, is given by

$$dx_s=\frac{\sum_{i=0}^{n}\frac{1}{D_{si}^2}\cdot dx_i}{\sum_{i=0}^{n}\frac{1}{D_{si}^2}} \tag{4}$$

where, dx_s, dx_i are, respectively, the displacement x-component of grid node and of i-th training point. D_{si} denotes the distance between the node and the i-th training point. n is the total number of training points.

2.3 Artificial Neural Networks

In the previous sub-section, we discussed briefly the classical approximation methods. In this sub-section, we focus our attention on two approximation methods based neural network, namely, GRNN and RBFNN.

2.3.1 Introduction to ANNs

The notion of artificial NN is inspired directly from the human brain as the biological model consisting of about 10^{11} nerve cells called neurons. Each neuron is connected by nerve fibres with approximately 10 000 neighbouring cells. A neuron can be compared with a simple processing unit, which receives an input, processes it and transmits an output to the following neuron (Schuh et al., 2002). From 1940s, the ANNs have been developed to solve practical problems. Today, with development of high-speed computation techniques, ANNs can be trained to solve more complex problems that are difficult for traditional methods.

A neural network model can be imagined as a system containing several layers with nodes (or neurons) in the layers. This network is characterized by one input layer, one or more hidden layers and one output layer (Figure 1). Each neuron in the hidden layer has one or more input data and one or more output data. The input information of the neuron is manipulated by

means of synaptic weights that are adjusted during a training process. After this procedure, a transfer (or activation) function is applied to all neurons for generating the output. According to Eq. 5, the output of the process (a) with a single output neuron may be expressed by

$$a = f\,(W\,p - b) \tag{5}$$

where W is the weight which describes the strength between the input p and output a, b is a bias. f is the activation function chosen by the designer. The most commonly used functions in ANNs are the linear, log-sigmoid and Gaussian functions.

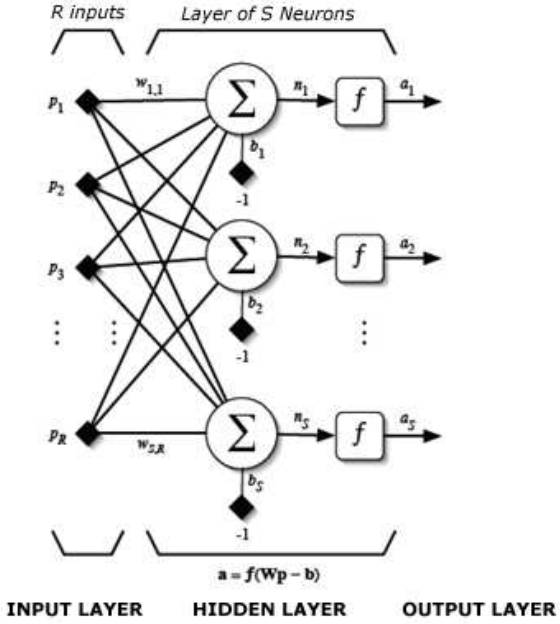

Fig. 1: Structure of a general neural network.

2.3.2 Generalized Regression Neural Network (GRNN)

The GRNN was introduced by Nadaraya and Watson and rediscovered by Specht (Specht, 1991) to perform general (Linear or non Linear) regressions. Unlike the RBF neural network, the training patterns are propagated through the network only once and consequently the training is achieved very quickly.

The topology of a GRNN is described in Figure 2 and it consists of four layers:

1. The input layer that is fully connected to the pattern layer.
2. The pattern layer that has one neuron is assigned for each training pattern. These neurons have radial basis activation functions (Gaussian functions) of the form:

$$\phi_i = exp\left(\frac{-D_i^2}{2\sigma^2}\right) \tag{6}$$

3. The summation layer has two units N and S. The first unit computes the weighted sum of the hidden layer outputs and the second unit has weights equal to 1, consequently is the summation of exponential terms ϕ_i alone.

4. The output unit divides *N* and *S* to provide the prediction result.

$$\hat{y} = \frac{\sum_{i=0}^{n} \phi_i \cdot Y_i}{\sum_{i=0}^{n} \phi_i} \tag{7}$$

For more details on the GRNN process, we refer the reader to (Abdul Hanna et al., 2010).

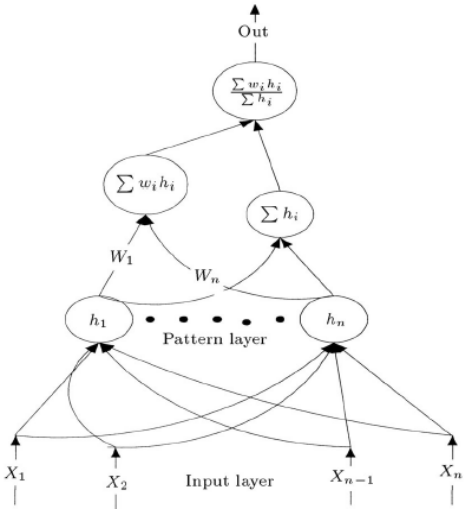

Fig. 2: The GRNN architecture.

From the previous formulations, we can see that the GRNN has only one parameter noted σ also called smoothing factor (SF) that needs to be determined. This factor provides a smooth transition from one observed value to another, even with sparse data in a multidimensional space. The success of the GRNN depends on the selection of appropriate values of SF (Wasserman, 1993). The optimum value of SF is determined after several runs in the training stage, according to the root mean square error (*RMSE*) of the estimate (Eq. 12), which must be kept at minimum. If a number of iterations pass with no improvement in the *RMSE*, so that SF is determined as the optimum one for that data set. While applying the network to a new dataset, increasing the SF would result in decreasing the range of output values (Specht, 1991). The GRNN networks evaluate each output independently of the other outputs; GRNN networks may be more accurate than back-propagation networks when there are multiple outputs. GRNN work by measuring how far given samples pattern is from patterns in the training dataset. The output that is predicted by the network is a proportional amount of all the output in the training dataset. The proportion is based upon how far the new pattern is from the given patterns in the training dataset.

2.3.3 RBF Neural Network

The RBF network is one of the possible solutions to the real multivariate interpolation problem. The basic technique provides an interpolating function witch passes through every data point: Consider a mapping from a *d*-dimensional input space to a one-dimensional target space *y*, where the data set consists of N points $\{x_i \in \mathbb{R}^n, i = 1..N\}$ with the corresponding

targets $\{y_i \in \mathbb{R}, i = 1..N\}$. An exact interpolation is achieved by introducing a set of *N* basis functions, one for each data point, and then setting the weights for the linear combination of basis functions.

$$F(x) = \sum_{i=1}^{N} w_i \cdot \phi(\|x - x_i\|) \tag{8}$$

where $\|.\|$ denotes the Euclidean norm. The radially symmetric function $\phi(.)$ which maps from $\mathbb{R}^+$ to $\mathbb{R}$ is called a radial basis function and w_i denotes the weight of the *i*th node. For the case of this study, Gaussian basis functions have been selected (Eq. 6). The structure of RBF Neural Networks is shown in figure 3.

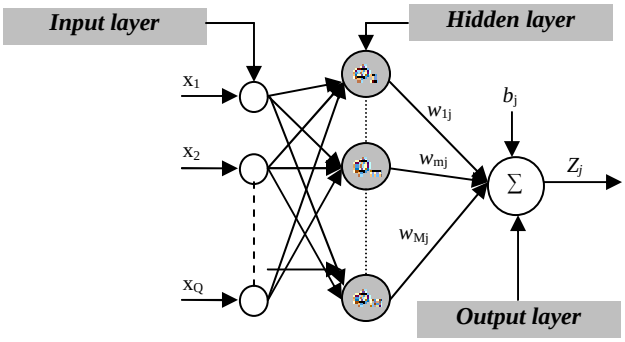

Fig.3: RBF architectural Neural Network

In this work, the learning of a RBF network is divided into two independently stages. In the first one, k-means clustering algorithm on the inputs data x have been employed to determine the parameters of the basis functions μ and σ. The second one is a supervised learning in which the weights and biases are determined and adjusted; this is done by minimizing mean square error E (Eq.11) between the desired outputs and calculated outputs.
Weights and biases are determined by the linear equations as follows:

$$w_{mj}^{i+1} = w_{mj}^{i} - \alpha \frac{\partial E}{\partial w_{mj}} = w_{mj}^{i} + \frac{\alpha}{M} \sum_{q=1}^{Q} [t_j^{(q)} - Z_j^{(q)}] \phi_m^{(q)} \tag{9}$$

$$b_j^{i+1} = b_j^{i} + \frac{\gamma}{M} [t_j^{(q)} - z_j^{(q)}] \tag{10}$$

Here *i* is the number of iterations, α and γ are the steps-size.
The mean square error E is given by:

$$E = \sum_{q=1}^{Q} \sum_{j=1}^{J} [t_j^{(q)} - Z_j^{(q)}]^2 \tag{11}$$

where $t_j^{(q)}$ is the desired output value of the *j-th* output neuron for the *q-th* input vector.

2.3.4 Evaluation of the performance of the proposed methods

In order to evaluate and to compare the performance of the proposed methods, two criterions were chosen in this end. The root mean square error (RMSE) given by:

$$RMSE = \sqrt{\frac{\sum_{i=1}^{n}\left(y_i - y_i^{'}\right)^2}{n}} \quad (12)$$

And the correlation coefficient given by:

$$\rho = 1 - \frac{\sum_{i=1}^{n}\left(y_i - y_i^{'}\right)^2}{\sum_{i=1}^{n}\left(y_i - \bar{y}\right)^2} \quad (13)$$

Where n is the number of estimate values, yi is the estimate value of the ith point, y'_i is the value of the reference point at the ith position and $\bar{y}$ corresponds to the mean of estimate values.

The interpolation method that yields the smallest value of RMSE and the biggest value of the correlation coefficient (ρ) is the best.

3. RESULTS AND DISCUSSION

3.1 Study Area

The liquefied Natural Gas (LNG) underground reservoir of the SONATRACH industrial enterprise (GL4/Z Complex – Arzew, Algeria), built in 1965, represented more than 50% of storage capacity of the complex. The prevention of industrial hazards, related to this reservoir, on the complex infrastructures and on the population of Arzew's town, has required a GPS monitoring network to perform a topographic auscultation of this important industrial site (figure 4).

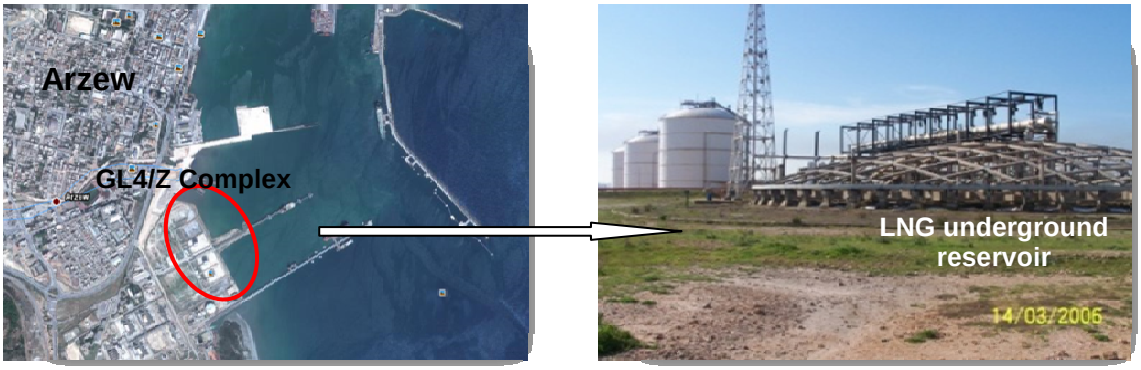

Fig. 4: Photos of the study area.

Four GPS observations campaigns were carried out, on February 2000, July 2002, July 2004 and February 2006. The GPS auscultation network, estimated with a precision of few millimetres, is composed of 15 reference points, 72 points for survey of reservoir neighbouring ground and 42 target points well distributed on the reservoir infrastructure. For this study, only data of 56 ground reservoir points were considered, over 6 year period (2000 – 2006).

3.2 GRNN Neural network construction

In the deformation process of the study area, the GRNN was implemented for the horizontal displacement field modelling of the GPS auscultation network of LNG reservoir as depicted in figure 5.

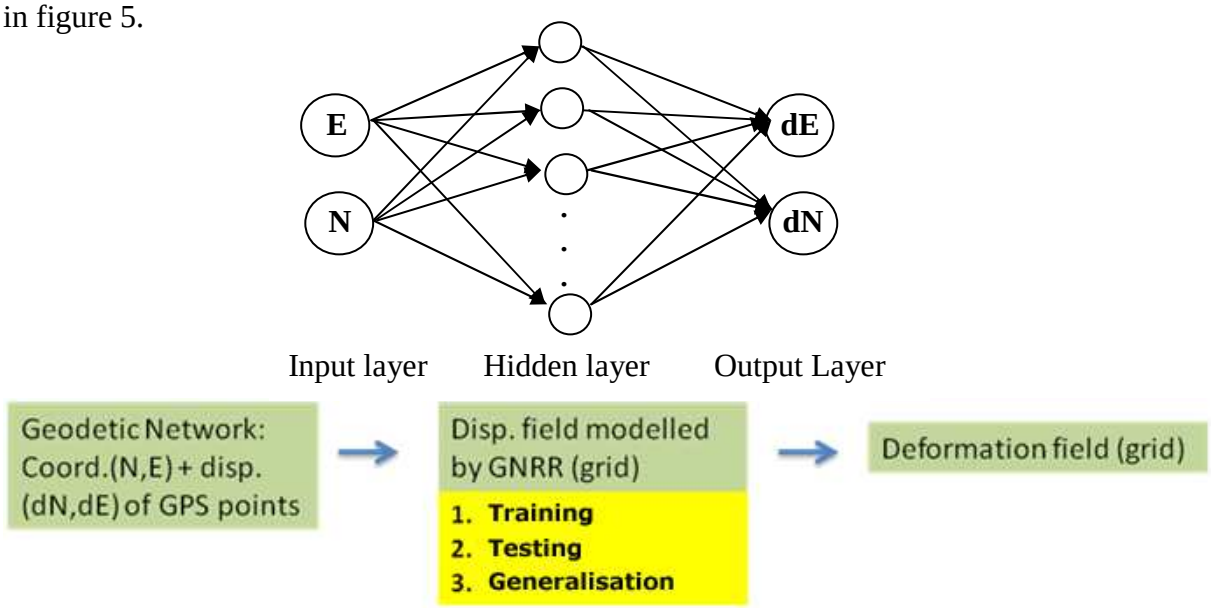

Fig. 5: Scheme of GRNN based Deformation process

The data are the local geodetic coordinates (*N*, *E*) of 56 GPS points and their derived displacements (*dN*, *dE*), over 6 year period. In order to test the efficiency of the method one part of the data is used for estimating the fitting model parameters (training set composed of 44 points, 79% of whole data set) and the other set is used for testing the model (testing set composed of 12 points, 21% of whole data set), as shown in figure 6. The generalisation is the final step for modelling the area displacement field which is employed to generate the deformation field according to a regular grid. The grid was composed of 304 meshes covering all the study area. Each mesh represents a surface of 10x10 m² on the ground.

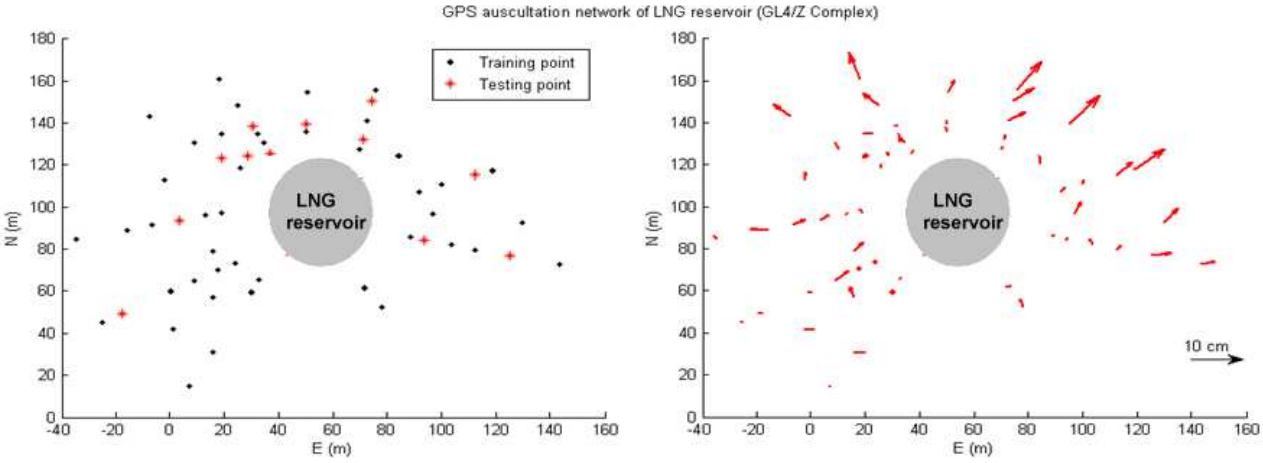

Fig. 6: Displacement vectors of the Auscultation GPS network of LNG underground reservoir.

3.3 Results and analysis

Since the most important feature of GRNN is referred to spread factor (SF), network has been trained with different SF until optimum value of SF can be determined. This later is chosen on basis of high correlation (close to 1) and high accuracy (minimum value of RMSE), according to the testing step. In this study, SF with a value of 15.0 has determined as optimum one. Table 1 depicts the obtained results of GRNN beside the correlation coefficient and RMSE of both training and testing steps. These results are illustrated by figure 7.

	ρ (Train) %		ρ (Test) %		RMSE (Train) mm		RMSE (Test) Mm	
SF	dE	dN	dE	dN	dE	dN	dE	dN
1	100.0	100.0	75.6	94.6	0.0	0.0	27.5	26.1
2	100.0	100.0	76.5	94.9	0.1	0.3	26.9	25.9
3	100.0	99.9	77.3	95.2	0.8	2.0	26.4	25.5
4	99.9	99.6	77.7	95.7	1.5	3.4	26.0	23.5
5	99.7	99.4	78.2	96.1	3.1	4.5	25.0	20.6
10	94.8	96.3	83.8	90.8	13.3	12.0	17.8	14.5
11	93.6	95.3	84.2	89.8	14.9	13.9	17.2	13.9
12	92.4	94.2	84.3	89.0	16.4	15.8	16.8	13.4
13	91.2	93.1	84.2	88.2	17.8	17.7	16.7	12.9
14	89.8	91.8	83.9	87.4	19.2	19.4	16.7	12.5
15	**88.4**	**90.4**	**83.6**	**86.7**	**20.5**	**20.9**	**16.9**	**12.2**
20	81.7	82.5	81.3	83.2	25.1	26.7	18.1	12.0

Table 1. GRNN performance results according to training and testing steps.

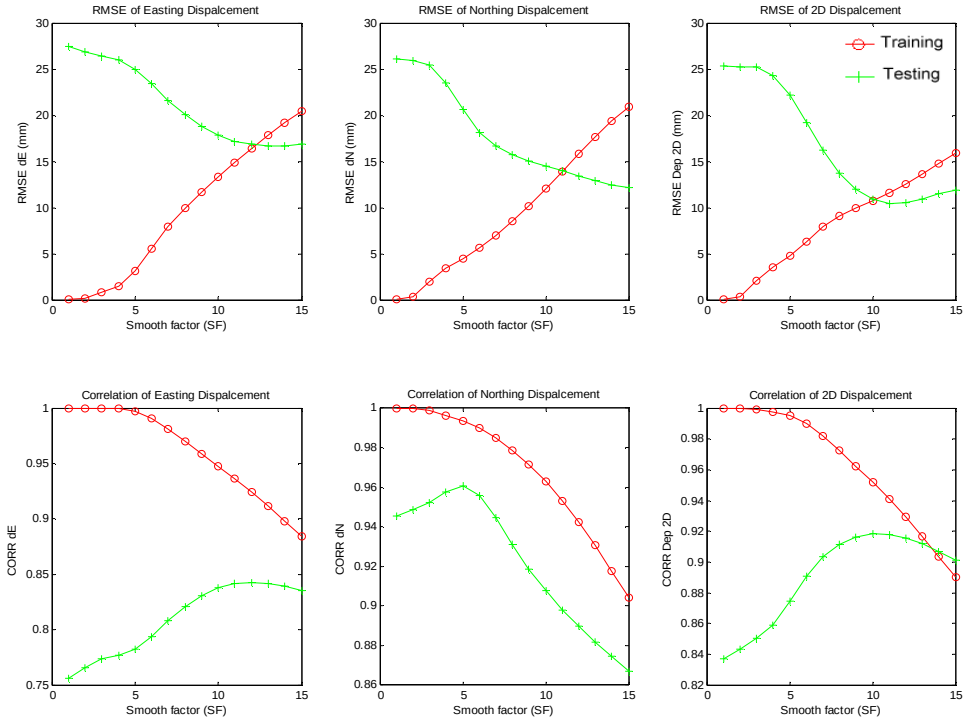

Fig. 7: Comparison between points displacements of training and testing steps according to RMSE and correlation parameters, in the case of GRNN neural network.

Figure 8 shows the displacement field obtained by the GRNN network.

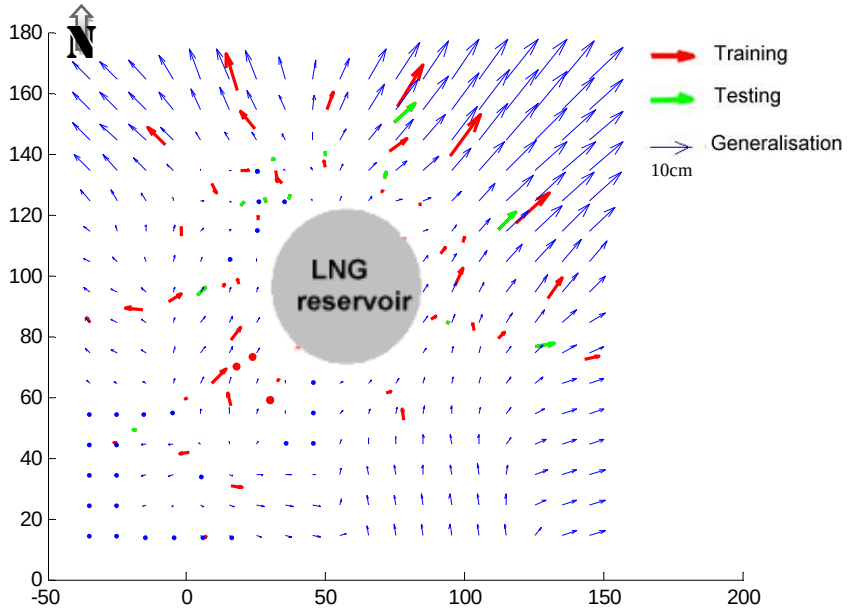

Fig. 8: Displacement field according to GRNN method with SF = 15.

The results of the second approximation approach based on RBFNN are listed in the table 2. Experiment has shown that best results are obtained for RBFNN with 23 hidden neurons, assuming the error evaluation was reached. From the table 2, the optimal SF value is 6. However, the figure 10 shows a discontinuous representation of the field displacements where the displacement vectors exist around and close to the measurement points. By choosing other value of SF, for example 20, depict of the displacement field is better even the according parameters performance are not optima.

	ρ (Train) %		ρ (Test) %		RMSE (Train) mm		RMSE (Test) Mm	
SF	dE	dN	dE	dN	dE	dN	dE	dN
1	98.5	98.8	-8.1	30.4	6.9	6.1	30.7	21.6
2	98.4	98.8	55.3	46.6	6.9	6.1	30.6	21.3
3	98.4	98.6	68.2	75.0	6.9	6.4	29.1	18.4
4	98.4	98.4	69.5	87.0	7.0	7.0	25.7	13.0
5	98.3	97.1	69.3	90.0	7.1	9.4	23.0	9.8
6	**98.2**	**96.9**	**69.2**	**90.5**	**7.5**	**9.7**	**22.2**	**9.7**
10	97.8	95.8	74.1	90.6	8.1	11.2	23.5	18.0
11	97.7	95.6	75.7	90.2	8.5	11.5	23.7	19.7
12	97.0	95.6	76.5	90.8	9.6	11.5	23.9	19.1
13	96.2	95.6	79.1	90.3	10.8	11.5	23.3	20.3
14	96.4	94.7	80.1	89.0	10.5	12.5	24.2	23.5
15	96.2	94.2	80.5	88.5	10.7	13.1	24.6	24.3
20	**92.6**	**92.9**	**83.6**	**92.8**	**14.8**	**14.5**	**21.4**	**21.0**

Table 2. RBFNN performance results according to training and testing steps.

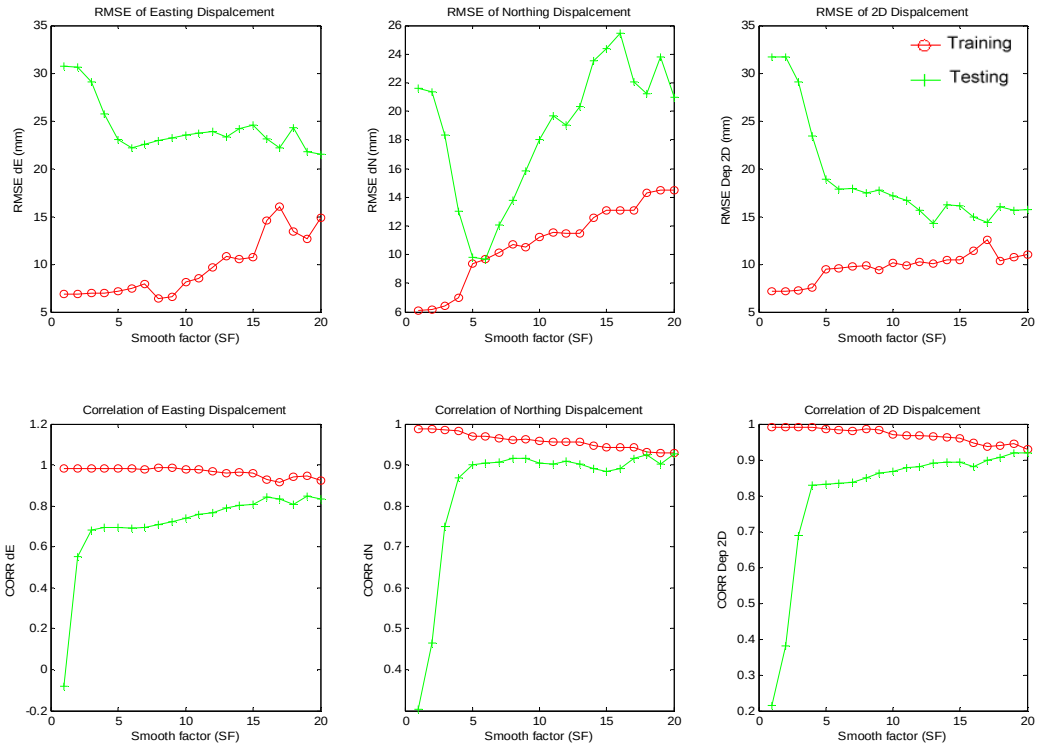

Fig. 9: Comparison between points displacements of training and testing steps according to RMSE and correlation parameters, in the case of RBFNN neural network.

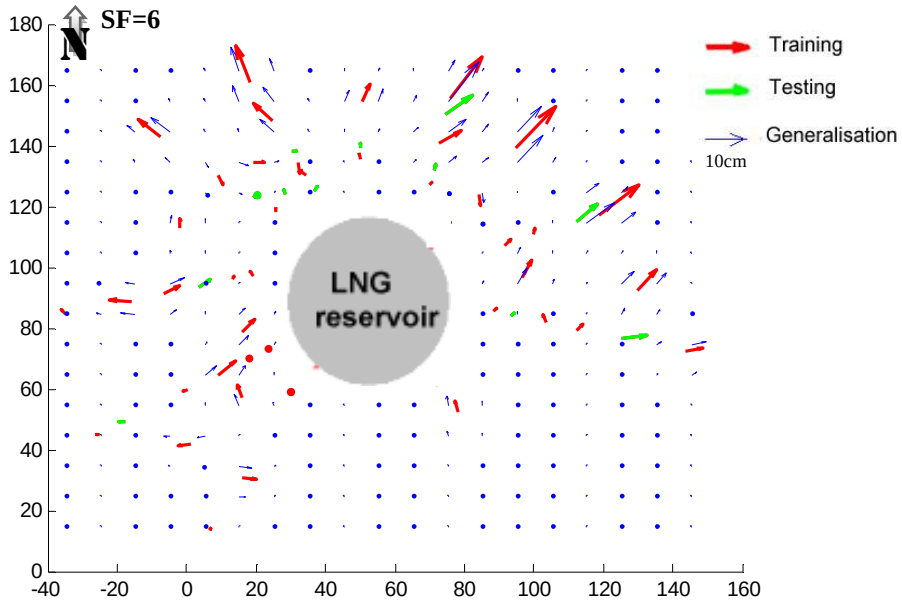

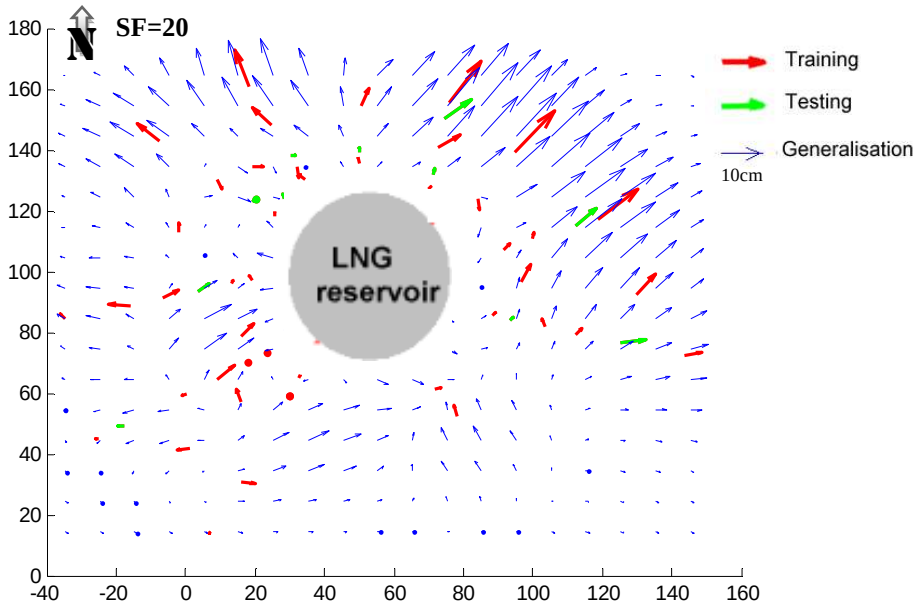

Fig. 10: Displacement field according to RBFNN method with Neurons number = 23.

In order to assess the accuracy of neural network approaches, the results of these methods will be compared to those of classical methods, namely Polynomial and Nearest Neighbour methods.

(a)	ρ (Train) %		ρ (Test) %		RMSE (Train) mm		RMSE (Test) mm	
Polynomial degree (PD)	dE	dN	dE	dN	dE	dN	dE	dN
2	68.1	52.8	59.0	73.3	28.8	33.3	25.7	14.9
3	76.6	71.7	74.5	89.8	25.3	27.3	22.3	13.6
4	**84.7**	**85.2**	**85.7**	**84.1**	**20.9**	**20.5**	**15.9**	**17.8**
5	88.1	92.3	61.4	80.7	18.6	15.1	27.9	18.1
6	97.4	96.6	54.9	49.0	9.0	10.1	29.7	13.9
7	95.4	95.7	45.1	-47.4	20.2	11.8	71.1	24.9

(b)	ρ (Test) %		RMSE (Test) mm	
Number of near neighbour points (NNP)	dE	dN	dE	dN
2	85.8	92.3	18.3	19.3
3	87.0	92.5	17.3	18.3
4	85.4	92.9	17.4	16.7
5	84.3	92.1	17.7	16.9

Table 3. Performance results according to (a) polynomial method (b) near neighbour method.

From the Table 3, we can see that the best approximation of the displacement field according to both RMSE and correlation factor computed on the dataset is obtained by the polynomial method with degree 4. This result corresponds to RMSE of about 15.9 and 17.8 mm, to correlation factor of about 85.7% and 84.1%, for easting and northing coordinates respectively.
To assess the performance of the GRNN network, a comparative evaluation against the RBFNN and polynomial method with degree 4 is performed. The comparison of results is summarized in Table 4.

Method	ρ(dE) %	ρ(dN) %	RMSE (dE) mm	RMSE (dN) mm
GRNN (SF=15)	83.6	86.7	16.9	12.2
RBFNN (SF=20) 23 hidden neurons	83.6	92.8	21.4	21.0
Polynomial (PD=4)	85.7	84.1	15.9	17.8

Table 4. Comparison between the performances of the three methods.

The performances listed in Table 4 show clearly that the GRNN outperform the RBFNN and the polynomial method. Using the GRNN, we obtain the RMSE of the displacement modulus of about 20.8 mm against to 23.9 mm and 30.0 mm in the case of polynomial and RBFNN methods respectively.

Figure 11 provides the representation of the deformation field of the LNG reservoir according to the strain tensors primitives, as described in section 2.1, with respect to the obtained displacement field from GRNN network with SF=15.
The dilatations/compressions are represented by circles with radii proportional to the amplitudes of deformations. It can be seen a dominant dilatation phenomenon that characterizes the auscultation network of the LNG reservoir, during 2000-2006 period. Large dilatations, at level of 3000–4700 ppm are located in the North and East of the reservoir while a weak compression is observed at its neighborhood in NW and SE directions. The shear expresses the change in configuration (e.g., a square becomes a lozenge). The shear value increases with increasing strain tensors; therefore, we have found regions of high deformation of about 1000–2000 ppm which are around the reservoir (North and East sides), except for the South and West sides where the shear is weak and at level of 200 ppm.
The twists are represented by vertical segments whose lengths correspond to rotations modules. The red and blue arrows are, respectively, positive and negative rotations. The maximum values are of about 790 dmgr.

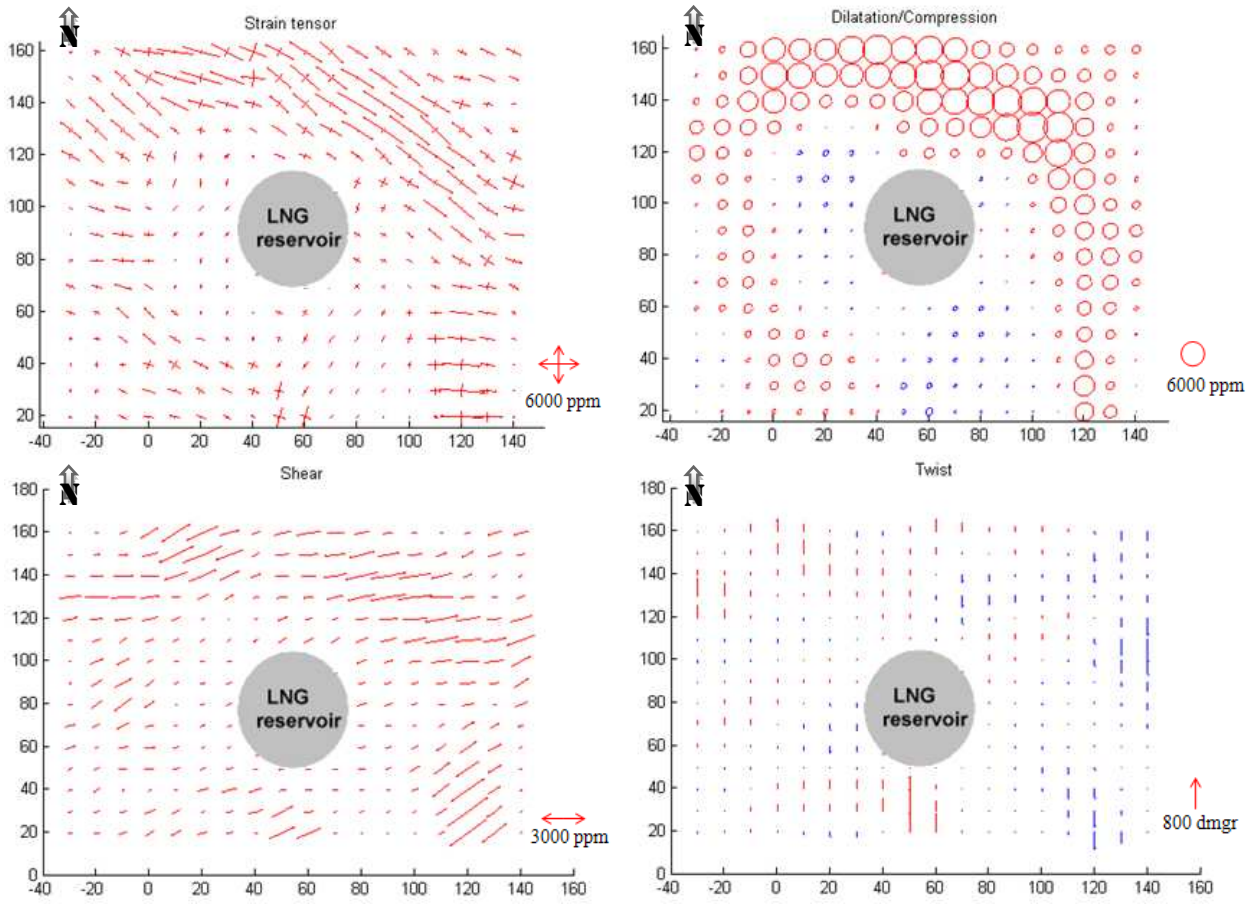

Fig. 11: Deformation primitives of the LNG reservoir auscultation network.

4. CONCLUSION

In this paper, the GRNN and the RBF Neural Networks were applied for horizontal displacement field modelling of GPS Auscultation Network of LNG reservoir. The preliminary experimental results demonstrated the potentials and the efficiency of the GRNN method compared to RBFNN and classical interpolations.

Future research will involve using the Least Vector Quantization (LVQ) method in order to perform a non supervised selection of the testing points and to extend this study for 3D displacement field modelling.

REFERENCES

Abdul Hanna S., R. R. Manza, R. J. Ramteke: Generalized Regression Neural Network and Radial BasisFunction for Heart Disease diagnosis. *International Journal of Computer Applications (0975 – 8887).* Volume 7– No.13, October 2010.

Gikas V., Sakellariou M.: Horizontal Deflection Analysis Of A Large Earthen Dam By Means Of Geodetic And Geotechnical Methods. 13th FIG symposium on Deformation measurement and analysis and 4th IAG symposium on Geodesy for geotechnical and structural engineering, LNEC, Lisbon 2008 May 12-15.

Gikas V., Sakellariou M.: Settlement analysis of the Mornos earth dam (Greece): Evidence from numerical modeling and geodetic monitoring. Engineering Structures 30 (2008) 3074–3081. doi:10.1016/j.engstruct.2008.03.019

Gullu Mevlut, Mustafa YILMAZ and Ibrahim YILMAZ: Application of Back Propagation Artificial Neural Network for Modelling Local GPS/Levelling Geoid Undulations: A Comparative Study. FIG Working Week 2011Bridging the Gap between Cultures, Marrakech, Morocco, 18-22 May 2011.

Kasser, M. et Thom, C. (1995). Etude des déformations dans un réseau géodésique par emploi de tenseurs de défomations régulièrement répartis.

Lin, L.S., 2009. Application of neural network and least squares collocation to GPS heighttransformation. Proceedings of ACRS 2009, Asian Association on Remote Sensing, Beijing, PRC. (http://www.a-a-r-s.org/acrs/proceeding/ACRS2007/Papers/TS37.6.pdf)

Merbah, A., B. Gourine, S. Kahlouche, M. Meghraoui, B. Ghezali and M. J. Sevilla (2005). Evaluation et Interprétation des Déformations Horizontale et de leurs Erreurs sur un Réseau de surveillance Sismique, *FIG Working Week 2005 and GSDI-8.*

Miima JB, Niemeier W, Kraus B (2001). A neural network approach to modelling geodetic deformations. In: Carosio, A., Kutterer, H. (Eds.), Proceedings of the 1st International Symposium on Robust Statistics and Fuzzy Techniques in Geodesy and GIS, Zurich, Swiss: pp. 111-116.

Moghtased-Azar Khosro and Piroska Zaletnyik: Crustal Velocity Field Modelling with Neural Network and Polynomials. International Association of Geodesy Symposia, 2008, Volume 133, Part 4, 809-816, DOI: 10.1007/978-3-540-85426-5_93

Prescott, W. H., Savage, J. C., and kinoshita, W. T. (1979). Strain accumulation rates in the western United States between 1970 and 1978. *J. Geophys. Res.*, 84, 5423-5435.

Schuh H, Ulrich M, Egger D, Muller J, Schwegmann W (2002). Prediction of Earth orientation parameters by artificial neural networks. J. Geodesy, 76: 247-258.

Seemkooei, A.A.(2001). Comparison of reliability and geometrical strength criteria in geodetic networks. *Journal of Geodesy* 75, 227-233.

Specht, D. F.: A General regression neural network. IEEE transactions on neural networks, vol. 2. No. 6, November 1993.

Taboli Hamid,Morteza Jamali Paghaleh,Asghar Afshar Jahanshahi, Raoof Gholami, Rashid Gholami : Specification and Prediction of Net Income using by Generalized Regression Neural Network (A Case Study). Australian Journal of Basic and Applied Sciences, 5(6): 1553-1557, 2011, ISSN 1991-8178.

Vaniçek, P., M.R. Craymer, E.J. Krakiwsky (2001). Robustness analysis of geodetic horizontal networks. *Journal of Geodesy* 75, 199-209.

Wasserman P.D., Advanced Methods in Neural Computing, Van Nostrand Reinhold, NewYork, USA, 155-161(1993).

Welsch, W. (1983). Finite element analysis of strain patterns from geodetic observations across a plate margin. *Tectonophysics.* 97, pp. 57-71.

BIOGRAPHICAL NOTES

Bachir GOURINE received an Engineer Diploma in *Geodesy* in 1994 at the National Centre of Spatial Techniques (CNTS, Arzew/Algeria) and obtained his Magister degree in *Space Techniques and Applications* at the Centre of Spatial Techniques (CTS), in 2004. During 2004, he is a permanent researcher at the Space Geodesy Division of CTS. On January 2011, he is PhD graduated in *Telecommunication*, Faculty of Electrical Genius, Department of Electronics - University Sciences and Technology Mohamed Boudiaf (USTO, Oran/Algeria). His research fields include: Space Geodesy, Geosciences Time series Analysis, Combination of space positioning systems data, Deformation modelling by neural networks, Adjustment of geodetic networks...

CONTACT

Centre des Techniques Spatiales (CTS)
Division de Géodésie Spatiale.
Arzew
ALGÉRIE
Tél. +213 41 472217
Fax. +213 41 473665.
Email: bachirgourine@yahoo.com

Habib Mahi received an Engineer Diploma in *Computer Science* in 1994 at the University of Mohamed Boudiaf (USTO) and obtained his Magister degree in *Techniques Spatiales et Applications* at the Centre of Space Techniques (CTS), Algeria in 2004. During 2004, he is a permanent researcher at the Earth Observation Division of CTS. His research interests include: image processing, image feature extraction and application of neural networks in remote sensing field.

CONTACT

Centre des Techniques Spatiales (CTS)
Division de l'Observation de la Terre
Arzew
ALGÉRIE
Tél. +213 41 472217
Fax. +213 41 473665.
Email: mahihabib@yahoo.fr

Amar KHOUDIRI and Youcef LAKSARI: obtained their Engineer Diploma in Geodesy on 2011 at Centre of Spatial Techniques (CNTS, Arzew/Algeria). They worked on application of the neural networks for deformation modelling of geodetic networks.